

Fraunhofer diffraction at the two-dimensional quadratically distorted (QD) Grating

YUEWEI LIU^{1,2,†} AND YAN FENG^{2,3,†,‡,*}

¹School of mathematics and statistics, Lanzhou University, Gansu, 730000 P. R. China.

²Institute of Biological Chemistry, Biophysics and Bioengineering, Heriot-Watt University, Edinburgh, EH14 4AS UK.

³Beijing National Laboratory for Molecular Sciences, Key Laboratory of Molecular Nanostructure and Nanotechnology, Institute of Chemistry, Chinese Academy of Sciences, Beijing, 100190 P. R.China.

[†]These authors contributed equally to this work.

[‡]Present address: Laboratory BioEmergences (USR3695), CNRS, University Paris-Saclay, Gif-sur-Yvette, 91198 France.

*Corresponding author: yanfeng4DMCMI@gmail.com.

Compiled December 14, 2024

A two-dimensional (2D) mathematical model of quadratically distorted (QD) grating is established with the principles of Fraunhofer diffraction and Fourier optics. Discrete sampling and bisection algorithm are applied for finding numerical solution of the diffraction pattern of QD grating. This 2D mathematical model allows the precise design of QD grating and improves the optical performance of simultaneous multiplane imaging system. © 2024 Optical Society of America

OCIS codes: (050.1970) Diffractive Optics; (050.1950) Diffraction Gratings; (110.4190) Multiple Imaging; (180.6900) Three-Dimensional Microscopy.

Using principles of adaptive optics, a novel simultaneous multiplane imaging system based on quadratically distorted (QD) grating was developed by Greenaway and Blanchard in 1990s [1], which was originally designed for photonic-crystal-fibre strain sensors and used in astronomy [2]. QD grating, which is also known as an off-axis Fresnel Zone Plate (FZP) [3], is formed by arcs of a series of concentric circles with varying radii as demonstrated in Figure 1. It behaves like a multi-focus ‘lens’ but utilizes principle of diffraction instead of refraction, and provides an order-dependent focussing power to generate several images. This simple, on axis and scanless imaging system can simultaneously capture multiple, in-focus specimen planes on a single image plane, and z-plane separations of multi-focal images can be varied from arbitrarily small to many microns. As an optical attachment, it is fully compatible with a commercial microscope and standard camera system.

A different implementation of similar principles, the so-called aberration-corrected multifocus microscopy (MFM), was developed by late Gustafsson and Abrahamsson [4]. It is capable of producing an instant focal stack of nine 2D images in multiple colours, and can be extended to image up to 25 focal planes under some circumstance [5]. However, the multifocus grating (MFG), which is one of the key optical elements and utilized to provide a variety of focal lengths (like QD grating), is designed by computer programming in a ‘black box’ instead of theoretical analysis [6]. Due to the technical ceilings, this customized optical system may only be appropriate for limited applications.

Due to the high level of sophistication in 2D mathematical modelling of quadratically distorted (QD) grating, in the past a rough one-dimensional (1D) model was built for the design and optimization of QD grating, in which the characteristic quadratic curvature and chirped-period were simplified as 1D equidistant slits [7]. In this paper, we will establish a 2D mathematical model of QD grating, calculate both analytical and numerical solutions of the Fraunhofer diffraction pattern, and finally verify this model.

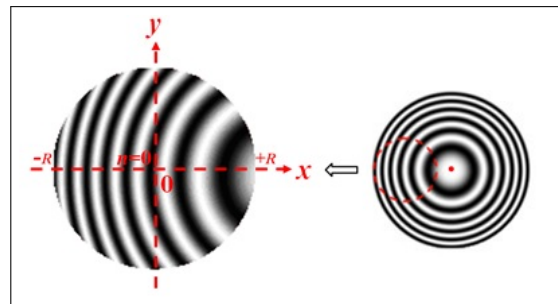


Fig. 1. A demonstration of the structure of QD grating in an x - y Cartesian coordinate system.

It has been proved that the scalar diffraction theory can be utilized for evaluating the image formed with a source of natural light by an optical system of moderate numerical aperture, thus

an approximate description in terms of a single complex scalar wave function is adequate to describe most problems encountered in optics [3]. The further approximation, which is referred to as Fraunhofer approximations, have greatly simplified the calculations of diffraction patterns under certain conditions. The evaluation of Fraunhofer diffraction could be written as a Fourier integral

$$U(p, q) = \iint_{\Omega} G(x, y) e^{-\frac{2\pi i}{\lambda}(px+qy)} dx dy, \quad (1)$$

where $G(x, y)$ is the QD grating function defined in the domain Ω and λ is the wavelength of the incident light. According figure 1, the QD grating function can be given as

$$G(x, y) = \begin{cases} e^{i\omega}, & \text{at points in the opening,} \\ 1, & \text{at points outside the opening,} \end{cases} \quad (2)$$

where $\omega \neq 0$ is the phase.

Three steps are applied to estimate the Fourier integral 1 of Fraunhofer diffraction: calculating the integral at a series of single circular sectors, approximating the integral in slits by the subtraction between adjacent sectors and summing all the integral in all slits with different phases. Supposing there are N arcs in the QD grating, the j th, $j = 1, 2, \dots, N$, single sector in the QD grating is plotted in figure 2. In this figure, δ_j is the angle and r_j is the radius of this sector. The start point a of the sector can be valued at $-1/2\delta_j$ because the sector is symmetric. Therefore, the integral in the sector is

$$U_j(p, q) = \iint_{\Omega} G_j(x, y) e^{-\frac{2\pi i}{\lambda}(px+qy)} dx dy, \quad (3)$$

where $G_j(x, y)$ is the j th sector with the j th arc in the grating function $G(x, y)$. When $G_j(x, y) = 1$, by a transformation to

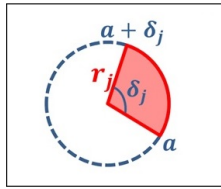


Fig. 2. A single circular sector in the QD grating.

poplar coordinate system in both the (x, y) plane and the (p, q) plane, (3) can be written as

$$\begin{aligned} F_j &= \frac{e^{ikz} e^{ik\rho^2/2z}}{i\lambda z} \int_0^{r_j} \int_a^{a+\delta_j} e^{i\frac{2\pi}{\lambda z} \rho r \sin(\theta-\phi-\frac{\pi}{2})} r dr d\theta \\ &= \frac{e^{ikz} e^{ik\rho^2/2z}}{i\lambda z} L \end{aligned} \quad (4)$$

where $k = 2\pi/\lambda$ is the number of waves, z the observation distance between aperture and image plane, and

$$\begin{aligned} r &= \sqrt{x^2 + y^2}, \quad \theta = \arctan(x/y), \\ \rho &= \sqrt{p^2 + q^2}, \quad \phi = \arctan(q/p) \end{aligned}$$

are the transformations from the (x, y) plane and the (p, q) plane to polar coordinates.

By Jacobi-Anger expansion,

$$e^{i\beta \sin \theta} = \sum_{n=-\infty}^{+\infty} J_n(\beta) e^{in\theta}, \quad (5)$$

where $J_n(\cdot)$ is the first kind Bessel function of order n , the integral L in (4) becomes

$$L = \sum_{n=-\infty}^{+\infty} \int_0^{r_j} J_n\left(\frac{2\pi}{\lambda z} \rho r\right) r dr \int_0^{\delta_j} e^{in(\theta+\psi)} d\theta \quad (6)$$

where $\psi = (a - \phi - \frac{\pi}{2})$. Because of $\int_0^x \zeta J_0(\zeta) d\zeta = x J_1(x)$, the middle term

$$L_0 = \frac{\delta_j \lambda z r_j}{2\pi \rho} J_1\left(\frac{2\pi}{\lambda z} \rho r_j\right) \quad (7)$$

for $n = 0$. Since the identity for the first kind Bessel function of order n , $J_{-n}(x) = (-1)^n J_n(x)$, we have the sum in (6)

$$L = L_0 + \left(\frac{2\pi}{\lambda z} \rho\right)^{-2} \sum_{n=1}^{+\infty} L_n, \quad (8)$$

where

$$\begin{aligned} L_n &= \int_0^{\frac{2\pi \rho r_j}{\lambda z}} r J_n(r) dr \int_0^{\delta_j} [e^{in\psi} + (-1)^n e^{-in\psi}] d\theta \\ &= \Psi_n \Phi_n \end{aligned} \quad (9)$$

Before calculating the first integral Ψ_n in (9) we introduce a result in [8]. Letting $\Gamma(\cdot)$ be the Gamma function, the result is following

$$\int_0^x t^\mu J_\nu(t) dt = x^\mu C \sum_{k=0}^{+\infty} C_k, \quad (10)$$

where

$$C = \frac{\Gamma\left(\frac{1}{2}\nu + \frac{1}{2}\mu + \frac{1}{2}\right)}{\Gamma\left(\frac{1}{2}\nu - \frac{1}{2}\mu + \frac{1}{2}\right)}, \quad (11)$$

and

$$C_k = (\nu + 2k + 1) \frac{\Gamma\left(\frac{1}{2}\nu - \frac{1}{2}\mu + \frac{1}{2} + k\right)}{\Gamma\left(\frac{1}{2}\nu + \frac{1}{2}\mu + \frac{3}{2} + k\right)}. \quad (12)$$

Letting $\mu = 1$ and $x = 2\pi \rho r_j / \lambda z$ in (10), the first integral Ψ_n in (9) is obtained

$$\Psi_{2m} = \frac{2\pi}{\lambda z} \rho r_j m \sum_{k=0}^{+\infty} \frac{2m + 2k + 1}{(m+k)(m+k+1)} J_{n+2k+1}\left(\frac{2\pi}{\lambda z} \rho r_j\right), \quad (13)$$

for an even number $n = 2m$ and

$$\begin{aligned} \Psi_{2m-1} &= 2(2m-1) \frac{2\pi}{\lambda z} \rho r_j m \cdot \\ &\sum_{k=0}^{+\infty} \frac{m+k}{(m+k+\frac{1}{2})(m+k-\frac{1}{2})} J_{n+2k+1}\left(\frac{2\pi}{\lambda z} \rho r_j\right), \end{aligned} \quad (14)$$

for an odd number $n = 2m - 1$.

The second integral Φ_n in (9) can be calculated directly and it is

$$\Phi_{2m} = \frac{2(-1)^m}{m} \sin(m\delta_j) \cos(m\delta_j - 2m\phi + 2ma) \quad (15)$$

for an even number $n = 2m$, and

$$\Phi_{2m-1} = \frac{4(-1)^m i}{2m-1} \sin\left[\frac{(2m-1)\delta_j}{2}\right] \cos\left[\frac{(2m-1)(\delta_j + 2a - 2\phi)}{2}\right], \quad (16)$$

for an odd number $n = 2m - 1$. Therefore, the integral in the j th sector is

$$F_j = \frac{e^{ikz} e^{ik\rho^2/2z}}{i\lambda z} \left[L_0 + \left(\frac{2\pi}{\lambda z} \rho \right)^{-2} \sum_{m=1}^{+\infty} (\Psi_{2m} \Phi_{2m} + \Psi_{2m-1} \Phi_{2m-1}) \right], \quad (17)$$

where $(L_0, \Psi_{2m}, \Psi_{2m-1}, \Phi_{2m}, \Phi_{2m-1})$ are defined in (7,13-16), respectively.

Now we estimate the integral in (1) with the integrals $F_j, j = 1, 2, \dots, N$, in all sectors. From figure 1 we know the grating consists of a lot of slits and each slit is bounded by \widehat{ABCD} as illustrated in figure 3. Seen in this figure, sectors \widehat{OAB} and \widehat{OCD} have different angles so slit \widehat{ABCD} cannot be approximated with the subtraction of the two sectors. A viable approximation of this slit is to construct a slit $\widehat{A'B'C'D'}$ closed to it. Specifically, we choose two point E, F in arc \widehat{AD} and arc \widehat{BC} , satisfying $OE = OF = 1/2(OA + OD)$, and extend arc \widehat{AB} and lines OE and OF , then we get the points of intersection of arcs $\widehat{AB}, \widehat{CD}$ and lines $\{OE, OF\}$. The angle δ_j of the sectors can be calculated as

$$\delta_j = 2 \arccos \left(\frac{r_0^2 + r_m^2 - R^2}{2r_0 r_m} \right), \quad (18)$$

where r_0 is the radius of the arc located at the center of the QD grating, $r_m = 1/2(r_j + r_{j+1})$ the radius of arc \widehat{EF} and R the radius of the QD grating. The integral in the slit $\widehat{A'B'C'D'}$ can be calculated by the subtraction of integrals in the two sectors $\widehat{OA'B'}$ and $\widehat{OC'D'}$. Therefore, the integral in (1) can be approximated by

$$U(p, q) = U(\rho \cos \phi, \rho \sin \phi) = \sum_{j=1}^n e^{i\omega \cdot \text{bool}} (F_{j+1} - F_j), \quad (19)$$

where the variable *bool* is equal to 1 if the slit in the opening, otherwise, it is zero.

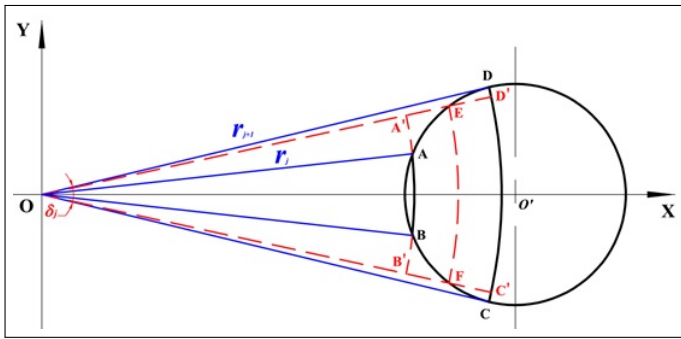


Fig. 3. Illustration of an approximation of a single slit in 2D.

In order to obtain quantity images the total image intensity should be equal in all diffraction orders. This intensity distribution depends on the phase so we attempt to determine a working phase which leads to a uniform distribution image intensity in the three orders under consideration. For a given phase ω , we denote $E(\omega) = \iint_{\Omega_I} |U((\rho \cos \phi, \rho \sin \phi))|^2 d\rho d\phi$ as the intensity function and $E_0(\omega) = \iint_{\Omega_{I_0}} |U((\rho \cos \phi, \rho \sin \phi))|^2 d\rho d\phi$ as the intensity function of zero order, where Ω_I and Ω_{I_0} are image

domain and zero order in the image domain. We construct the function as following

$$C(\omega) = \frac{1}{3} E(\omega) - E_0(\omega), \quad (20)$$

and then the working phase is the root of $C(\omega)$.

Since the intensity function is continuous with respect to the phase ω , the bisection algorithm can be applied to find the working phase. For a given tolerance ϵ , and two initial phases ω_1, ω_2 , which is subject to $C(\omega_1)C(\omega_2) < 0$, the algorithm is

Algorithm 1. The bisection algorithm

- 1: **while** $|\omega_1 - \omega_2| > \epsilon$ and $C(\omega) \neq 0$, where $\omega = \frac{\omega_1 + \omega_2}{2}$, **do**
- 2: **set**

$$\omega_1 = \omega, \text{ if } C(\omega_1)C(\omega) > 0$$

$$\omega_2 = \omega, \text{ otherwise}$$
- 3: **return** ω . ▷ The root is ω

The above algorithm is applied to a 2D QD grating with designed parameters listed in Table 1. In this table W_{20} is the

Table 1. Designed parameters of the 2D QD grating

Paramters	Value
Central Period (d_0)	50 μ m
Radius (R)	10mm
W_{20}	50 λ
Wavelength (λ)	532nm
Number of arcs	801

standard coefficient of defocus and is equivalent to the extra path length introduced at the edge of the aperture. With the parameter W_{20} , the non-period varying radii r_j can be obtained

$$r_j = \left[\frac{j\lambda R^2}{W_{20}} + \left(\frac{\lambda R^2}{2d_0 W_{20}} \right)^2 \right]^{1/2}. \quad (21)$$

The optimized working phase of the QD phase grating is found to be 1.99999rad based on the parameters shown in Table 1, hence the etch depth could be 368nm @532nm wavelength when the fused silica is applied as grating substrate. For comparison, we apply another 2D QD phase grating of the same design but with the phase of 2.00777rad which leads to slits with a same width. In Figure 4, the normalized intensity distribution of optimal QD phase grating is displayed in the form of contour plot due to the big difference of intensity maxima among the spots. The result for the phase of 2.00777 presents that the total normalized intensity in zero order and in $\pm 1^{\text{st}}$ orders are 0.329536266 and 0.335231867, respectively, which shows there is a small difference of intensity distribution compared to the optimized working phase. However, according to our modeling experience, the working phase may depend strongly on the curvature parameter(s) of QD grating, i.e. W_{20} . Consequently, the optimized phase of a considerable curved QD grating may be quite different with the value calculated by 1D model. For designs of high-quality QD grating, obtaining a precise working point should be essential.

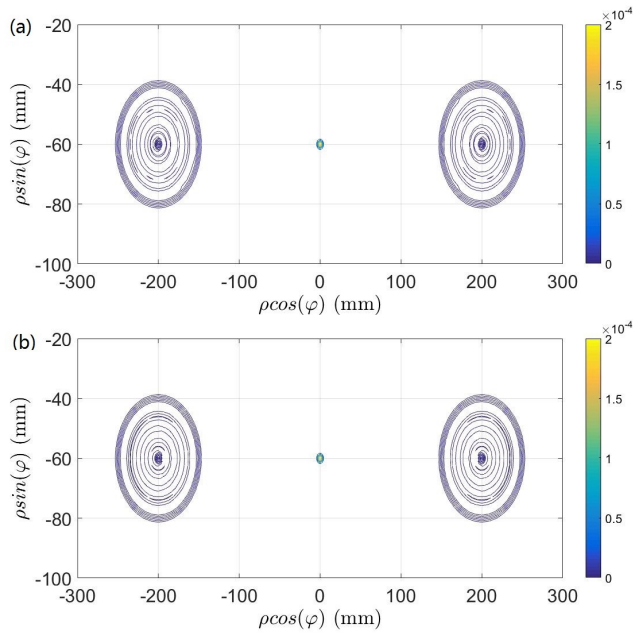


Fig. 4. Contour plot of normalized intensity for Fraunhofer diffraction pattern of 2D QD phase gratings with working phases of (a) 1.99999rad; (b) 2.00777rad.

In order to assess the validities and feasibilities of our calculation, a 2D grating model by quasi-straight-line QD grating is designed. The parameters of this grating are listed in Table 2. The parameter $W_{20} = 0.5\lambda$, makes that this grating looks almost straight. The optimized working phase by Algorithm

Table 2. Parameters of the quasi-straight-line QD grating

Parameters	Value
Central Period (d_0)	50 μ m
Radius (R)	10mm
W_{20}	0.5 λ
Wavelength (λ)	532nm
Number of arcs	800

1 is 2.00831rad, which is quite close to 2.00777rad the rough phase attained from a 1D and period-fixed QD grating model. The contour plots of Fraunhofer diffraction pattern is shown in Figure 5. From this figure, we see that the integrated intensity of first three orders is balanced with the working phase of 2.00831rad, which verifies both the 2D grating model as well as the numerical algorithm. Moreover, because of the central period of this quasi-straight-line 2D QD grating is equal to the period of the straight-line and period-fixed grating, we compare the Fraunhofer patterns of the two gratings and found that the peaks of both diffraction patterns locate at the same position which are exactly the theoretical ones.

Although the physical principles underlying the quadratic curves of off-axis Fresnel zone plate have been substantially formulated by Blanchard and Greenaway, it is, in some cases, not straightforward for practical use because the 'working' phase (thus the etch depth) of the QD grating is obtained from a very

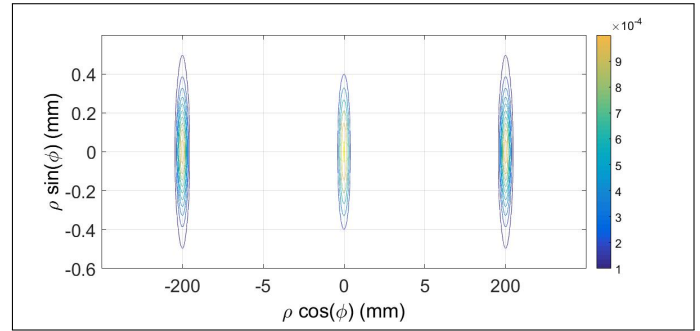


Fig. 5. Contour plot of normalized intensity for Fraunhofer diffraction pattern of the quasi-straight-line QD grating.

rough 1D period-fixed (i.e. equally spaced) grating model. In this paper, a description of Fraunhofer diffraction at the 2D QD grating in terms of an elaborate analytical model is first systematically established. Based on scalar diffraction theories and discrete uniform sampling method, the detailed energy distribution of QD grating has been demonstrated in a simple and graphic manner. This 2D theoretical model ensures that all the energy flow of incident light can be diffracted into first three diffraction orders, and an optimized working phase obtained by bisection method allows the integrated light intensity of each order to be balanced. This mathematical model of 2D QD grating is designed not only for current use of obtaining an accurate working phase as fabrication guide, but also for versatile design and further explorations of both QD grating and 4D imaging system.

REFERENCES

1. P. M. Blanchard and A. H. Greenaway, *Applied Optics* **38**, 6692 (1999).
2. A. Greenaway, *Physics World* **23**, 33 (2010).
3. M. Born and E. Wolf, *Principles of optics* (Cambridge University Press, 2001), corrected reprint of the 7th edition ed.
4. S. Abrahamsson, J. Chen, B. Hajj, S. Stallinga, A. Y. Katsov, J. Wisniewski, G. Mizuguchi, P. Soule, F. Mueller, C. Dugast Darzacq, X. Darzacq, C. Wu, C. Bargmann, D. A. Agard, M. Dahan, and M. G. L. Gustafsson **10**, 60 (2013).
5. S. Abrahamsson, M. Mcquillen, S. B. Mehta, A. Verma, J. Larsch, R. Ilic, R. Heintzmann, C. I. Bargmann, A. S. Gladfelter, and R. Oldenbourg, *Optics Express* **23**, 7734 (2015).
6. S. Abrahamsson, R. Ilic, J. Wisniewski, B. Mehl, L. Yu, L. Chen, M. Davanco, L. Oudjedi, J. B. Fiche, and B. Hajj, *Biomedical Optics Express* **7**, 855 (2016).
7. Y. Feng, A dissertation for the degree of Doctor of Philosophy, Precision Instruments and Machinery, University of Science and Technology of China, Hefei, China (2013).
8. <http://dlmf.nist.gov/10.22#E7>.